JOURNAL OF PHYSICAL ORGANIC CHEMISTRY
J. Phys. Org. Chem. 2007; **20:** 838–844
Published online 27 July 2007 in Wiley InterScience
(www.interscience.wiley.com) DOI: 10.1002/poc.1214

Photodimerization of soluble tetracene derivatives using visible light

Alexandre G. L. Olive,[1] André Del Guerzo,[1]* Jean-Luc Pozzo,[1] Jean-Pierre Desvergne,[1] Jens Reichwagen[2] and Henning Hopf[2]

[1]Institut des Sciences Moléculaires (ISM), Université Bordeaux 1, CNRS UMR 5255, 351 cours de la Libération, F-33405 Talence, France
[2]Institut für Organische Chemie, T.U. Braunschweig, Postfach 3329, D-38023 Braunschweig, Germany

Received 31 January 2007; revised 30 March 2007; accepted 12 April 2007

ABSTRACT: 2,3-Didecyloxytetracene (2,3-DDOT) is a yellow-orange soluble derivative that undergoes a strong de-coloration upon irradiation with visible light (470 nm). This is due to a photoreaction ($\Phi_r = 5.9 \times 10^{-3}$) that leads to the formation of four photodimers, involving only the two central rings of the tetracene core. Copyright © 2007 John Wiley & Sons, Ltd.
Supplementary electronic material for this paper is available in Wiley InterScience at http://www.mrw.interscience.wiley.com/suppmat/0894-3230/suppmat/

KEYWORDS: tetracene; photochromism; photodimer; photochemistry

INTRODUCTION

Anthracenes are well known to display photochromic properties. The photodimerization occurs upon irradiation with near UV light (<400 nm) and results in a blue shift (*ca*. 100 nm) of the absorption spectrum, whilst the back reaction (photocleavage) generating the starting material requires shorter excitation wavelengths (<300 nm).[1]

Tetracene shows comparable properties,[2] but has been less studied mainly because of its poor solubility in the usual solvents and organic matrices. Currently, only very few tetracene derivatives have been prepared due to their non-straightforward syntheses and moderate solubility, hampering their development in the fields of high density information storage or molecular electronics.[3,4] Nevertheless, these compounds are of interest because they offer a strong absorption in the visible range, in contrast to anthracenes which usually absorb mainly in the near UV range, and are expected to form photodimers upon visible light irradiation exhibiting a large hypsochromic shift (from visible to UV range) due to the formation of naphthalene chromophores. In addition, the photoreactivity of the tetracene core is not well known especially in relation with the nature and the position of the substituent(s) which for symmetry, electronic, or steric reasons affects the reaction pathways. In the present paper we report the photoreactivity of a 2,3-tetracene derivative that is fairly soluble in various solvents and is furthermore able to self-assemble into organogel fibers under certain conditions.[3b] The characterization and stability of the photoproducts are also reported.

**Correspondence to:* A. Del Guerzo, Institut des Sciences Moléculaires (ISM), Université Bordeaux 1, CNRS UMR 5255; 351 cours de la Libération, F-33405 Talence, France.
E-mail: a.del-guerzo@ism.u-bordeaux1.fr

RESULTS

When a sample of 2,3-didecyloxytetracene (2,3-DDOT; see synthesis, NMR and HRMS in Reference 3b) in cyclohexane is irradiated for 24 h by visible light, a bleaching of the solution was observed. Four photodimers were isolated by column chromatography as the major products. Although a fifth photoproduct was detected by TLC in trace amount, it could not be isolated and characterized. The photoproducts were isolated as oils or waxy solids and were stable over months, but no single crystals could be obtained, preventing thus X-ray analysis. The characterization by mass spectrometry or elemental analysis did not meet with success either, as already experienced previously with *n*-acene photoproducts.[1,3,5] Hence, the structures of the photodimers were determined by one- and two-dimensional NMR spectroscopy and supported by electronic absorption spectroscopy.

From ^{1}H, ^{13}C, HSQC, and HMBC NMR experiments, all the resonance signals in each four isolated photodimer were fully and unambiguously assigned (see Scheme 1 for the numbering of protons and experimental section). In the four photodimers, the ^{13}C NMR signals of the carbon

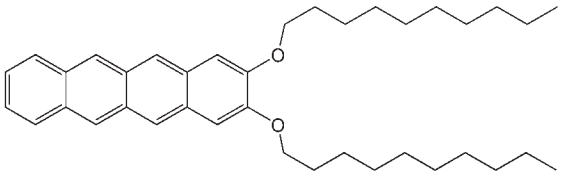

2,3-DDOT

syn- photodimers

anti-photodimers

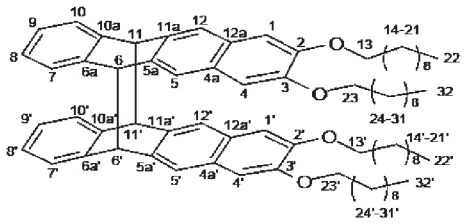

D1

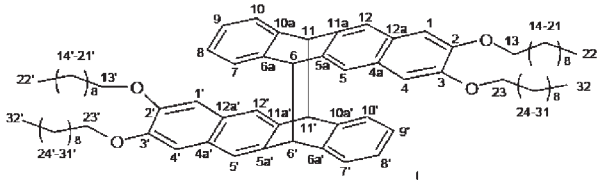

D3

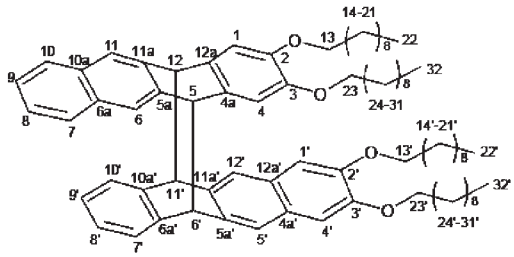

D2

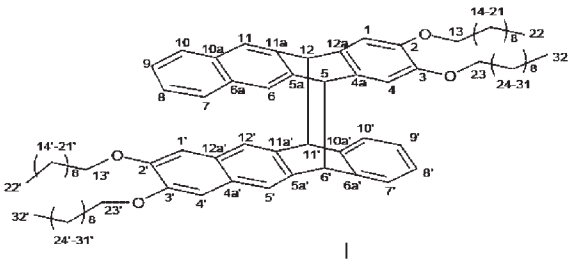

D4

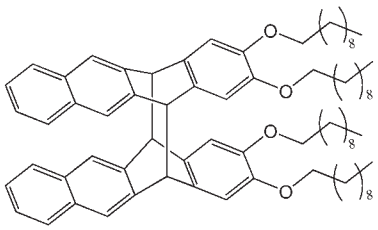

D5 (not detected)

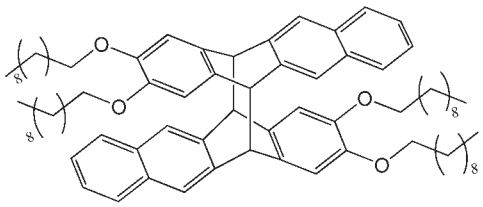

D6 (not detected)

Scheme 1. The six expected photodimers involving the tetracene central rings

in position C-2/3 (singlets) are the most deshielded because of their substitution with oxygen atoms, and thus can be safely attributed. As shown by HMBC NMR, these carbons are the sole to be correlated to the O—CH_2 of the alkoxy chain. Similarly, due to the proximity of oxygen, the protons H-1/4 are expected to be the most shielded ones (this is confirmed *a posteriori* for **D1**, **D2**, and **D4**). The attribution of the protons H-1/4 is confirmed by the correlation observed in HMBC NMR with the C-2/3. In ^{1}H NMR, all the protons display a singlet except the protons H-7/10 and H-8/9 (doublets, ^{1}H–^{1}H coupling constant is typically about 8.7 Hz). The signals of the protons H-7/10 and H-8/9 are clearly observed, as well as those of the protons H-1/4. This proves that the aromaticity of the terminal rings (^{1}H in positions 1, 4, 7, 8, 9, and 10) is preserved in all the photoproducts and are thus not directly involved in the photocycloaddition reaction. Thus, only six possible photodimers can theoretically be expected from reactions resulting from a 4 + 4 cycloaddition of the central rings (Scheme 1). Three photodimers can be classified as *syn* (head-to-head), whereas the three others as *anti* (head-to-tail) photodimers. Among these two subgroups, the cycloaddition can either involve the same ring of both subunits (two cases each) resulting in plano- or centrosymmetric compounds, or two different rings (non-symmetric).

DOI: 10.1002/poc

NMR reveals the symmetry of two photoproducts, as they present in the aromatic region only four signals in ^{1}H NMR and eight in ^{13}C NMR (Figure 1). These spectra thus correspond to photodimers of structure **D1**, **D3**, **D5**, or **D6**. In contrast, the two other photodimers display double the amount of signals, and can thus be attributed to the two possible non-symmetric photodimers of structure **D2** and **D4**.

The symmetric photodimers display a correlation of the protons H-7/10 and H-8/9 with the most proximal ternary carbon C-6a/10a, as found by HMBC NMR. The next proximal correlation of C-6a/10a occurs with the protons H-6/11, which are in this case the non-aromatic bridgehead protons.[3a] Since the cycloaddition involved de-aromatization of protons H-6/11 and H-6′/11′ and formation of C—C bonds C-6-6′ and C-11-11′, we can conclude that only **D1** and **D3** are formed, whereas **D5** and **D6** are not detected. The distinction between *syn* and *anti* photodimers is discussed later. The successive analysis of HMBC, HSQC, and one-dimensional NMR signals allows to precisely assign the other signals.

In the case of the non-symmetric photodimers **D2/D4** (Figure 2), in the first unit the carbon C-6a′/10a′ correlates with the protons H-7′/10′, H-8′/9′, and H-6′/11′. In this case, protons H-6′/11′ are non-aromatic. Similarly, in the case of the signals of the second unit, the carbon C-6a/10a correlates with the protons H-7/10, H-8/9, and H-6/11. In contrast to the first unit, the protons H-6/11 in the second unit are aromatic. This implies that the cycloaddition involves the formation of the C—C bonds between 5-6′ and 12-11′ vertices, respectively.

In order to definitely differentiate between the photodimer pairs **D1/D3** and **D2/D4**, we have used different experimental data. In a unique case, with the photodimer **D4** (Figure 2), a ROESY experiment has afforded a through-space ^{1}H–^{1}H correlation. The interaction occurs between the protons H-1/4 (resp. H-1′/4′) and H-7′/10′ (resp. H-7/10). This clearly indicates that **D4** corresponds to the non-symmetric *anti* photodimer. Thus, **D2** corresponds to the non-symmetric *syn* photodimer.

In order to confirm this attribution, and distinguish all the photodimers, we have also analyzed the shielding ring-current effects of the naphthalene core of one unit on the protons H-8/9 (or H-8′/9′) of the other unit. Knowing the structure of **D2**, we can indeed observe that the protons H-8′/9′ are situated above the *center* of the naphthalene core and shielded by 0.65 ppm as compared to the non-affected protons H-8/9 (6.62 *vs*. 7.27 ppm) (see structures in Scheme 1 and summary of chemical shifts in Table 1). In the case of the **D4** photodimer, the difference is smaller (0.38 ppm) and protons H-8/9 are barely shielded (7.18 ppm). This is linked to the fact that the protons 8/9 are off-centered relatively to the opposite naphthalene core. The protons H-8′/9′ (6.80 ppm) are shielded by the opposite, structurally close benzene core including the carbons C-2/3.

A similar analysis allows to distinguish between the photodimers **D1** and **D3**. Indeed, the protons H-8/9 (H-8′/9′) of the photodimer **D3** have a chemical shift of 6.59 ppm, similar to that of H-8′/9′ of **D2** (6.62 ppm), clearly demonstrating the shielding due to the opposite naphthalene core. The structure **D3** can thus be attributed to the symmetric *anti* photodimer. For the last compound **D1**, the protons H-8/9 (H-8′/9′) have chemical shifts of 6.81 ppm, identical to those of H-8′/9′ of **D4** (6.80 ppm). **D1** is thus the symmetric *syn* photodimer. A supplementary confirmation can be obtained by comparative analyses of the absorption spectra of the photodimers.

UV–Visible absorption spectroscopy is the classical technique to characterize the yellow-orange colored tetracene derivatives and their photochromic properties. Upon irradiation, a solution of monomer is bleached in the visible region of the spectrum (Figure 3, top) since the photodimers are uncolored and absorb in the UV range. Similar spectroscopic variations had also been observed during the photodimerization of the 5,12-DDOT derivative.[3a,c] This is related to the loss of aromatic conjugation over the four rings upon photodimerization, resulting in absorption patterns closely related to those of naphthalene. At the lowest energies, two weak absorption bands are observed around 320 and 350 nm (Figure 3, bottom). These bands were attributed to the $^{1}L_{b}$ transition of the naphthalene cores.[6] At higher energies, the photoproducts display a very strong absorption in which two components at 230 and 255 nm may be distinguished, with relative intensities depending on the photodimer structure (Figure 3). These contributions are due to the longitudinal transitions of the naphthalene cores.[6] It appears that for

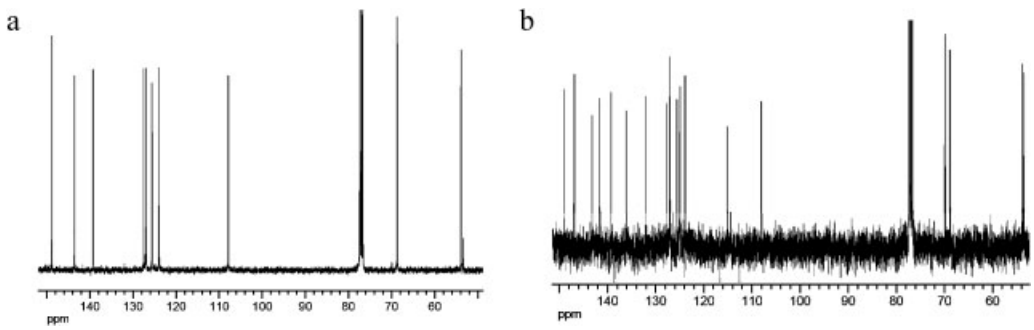

Figure 1. (a) ^{13}C NMR spectrum of **D1** (symmetric); (b) ^{13}C NMR spectrum of **D2** (non-symmetric) ($CDCl_3$, RT). Complete assignment of the signal is reported in the experimental section

DOI: 10.1002/poc

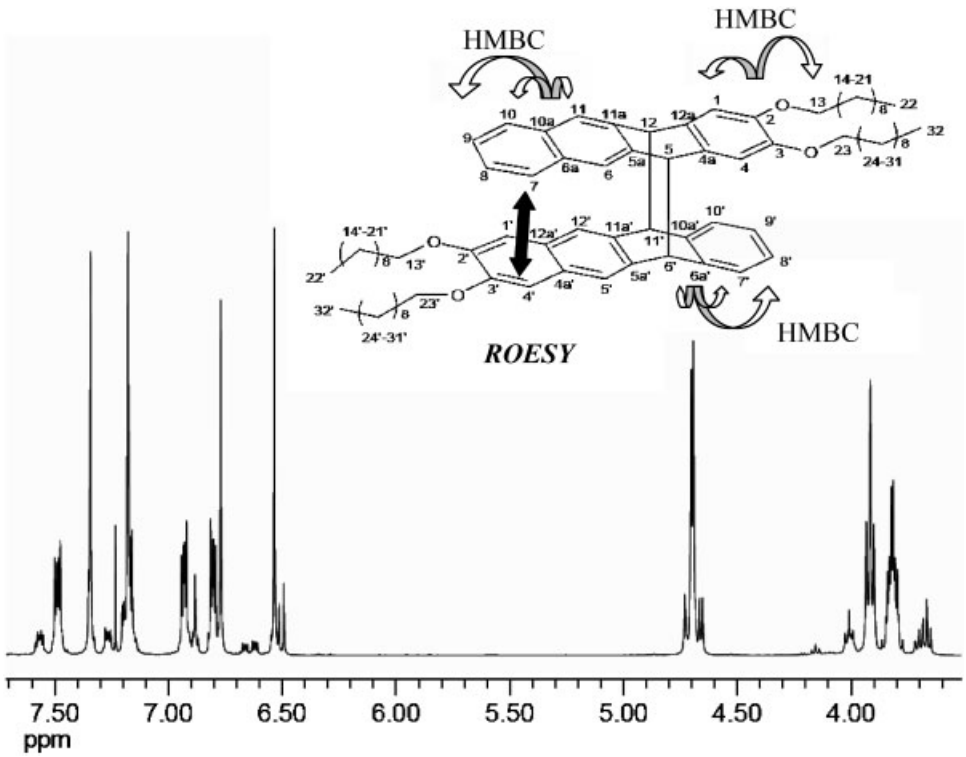

Figure 2. ^{1}H NMR spectrum of **D4** (non-symmetrical) ($DCCl_3$, RT). Curved arrows indicate the main HMBC correlations (see text). The black arrow indicates the ROESY correlation in **D4**

D3 and the *anti* photodimer of 5,12-DDOT the higher energy band (around 230 nm) is weak and not directly observed.[3a] These two photodimers are the only centro-symmetric compounds, suggesting that the transition at 230 nm is weakened due to the symmetry. In the case of **D3**, **D2**, and the *anti* photodimer of 5,12-DDOT, the band at 255 nm is clearly visible. In contrast, for **D1**, **D4**, and the *syn*-photodimer of 5,12-DDOT the equivalent band is weak or shifted to lower wavelengths. This suggests a coupling of the longitudinal dipolar transition moments of the naphthalene cores. Indeed, the structures of the latter photodimers clearly indicate that the naphthalene cores are sufficiently close and well aligned, favoring the phenomenon. In agreement with the above attributions of the UV absorption, the fluorescence exhibited by the photodimers (see supporting information) is characteristic of the naphthalene chromophore.

The photoreaction quantum yields Φ_r (measured in degassed medium) were found in fluid solution to be 5.9×10^{-3} and very similar to that obtained for the 5,12 derivative ($\Phi_r = 6.5 \times 10^{-3}$).[3a] The di-substitution pattern does thus not significantly change the reactivity of the tetracene chromophore. This value is also very close to that of the photodimerization of a comparable anthracene derivative, 1,4-didecyloxyanthracene ($\Phi_r = 6.5 \times 10^{-3}$).[7] In contrast to the photodimers obtained from the 5,12 derivative, the *syn* and *anti* photoproducts were unexpectedly found to be photostable under our experimental conditions and did not reverse to the starting material (2,3-DDOT). In addition, they display a good thermal stability as they only slowly form the 2,3-DDOT monomer upon heating of a toluene solution at 80 °C for several hours.

DISCUSSION AND CONCLUSION

As expected, the photocycloaddition occurs exclusively with the two central rings of the tetracene core. This has already been observed with non-substituted tetracene,[2] and generally with anthracene,[1] and is in correlation with the electronic density on the two vertices of the central

Table 1. Chemical shifts of 8/9 (or 8′/9′) protons in the four isolated photodimers

	D1	D2	D3	D4
Attribution	*Syn*/symm	*Syn*/non-symm	*Anti*/symm	*Anti*/non-symm
δ 8/9 (ppm)	6.81	7.27	**6.59**	7.18
δ 8′/9′ (ppm)	6.81	**6.62**	**6.59**	6.80

Note the important shielding observed for **D2** (H-8′/9′) and **D3** (H-8/9 and H-8′/9′), shown in bold.

DOI: 10.1002/poc

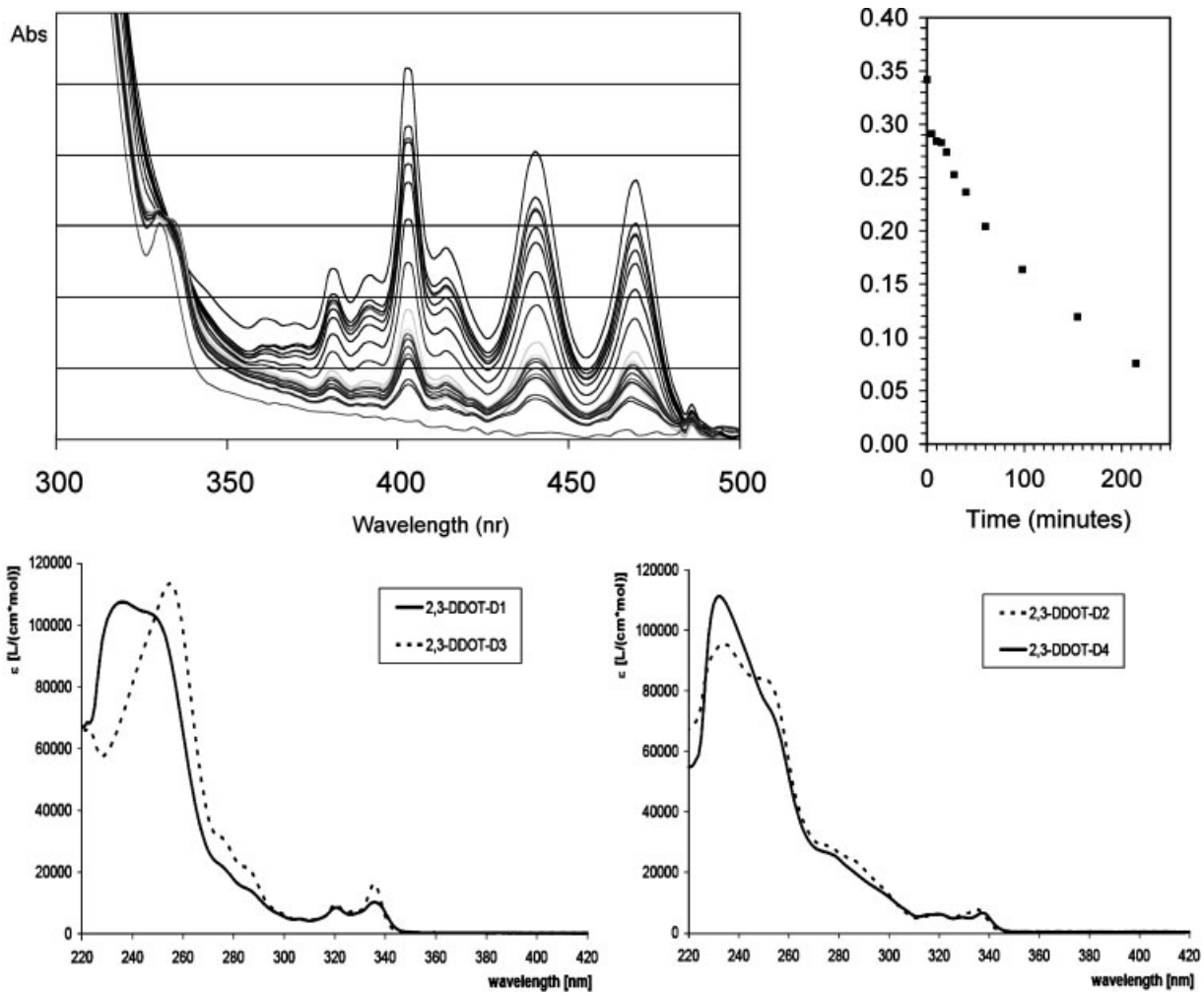

Figure 3. (Top) Evolution of the absorption of 2,3-DDOT upon irradiation at 470 nm (5 nm bandwidth) with increasing time, from 0 to 215 min: (left) electronic absorption spectrum, (right) O.D. at 470 nm. Note the decrease of tetracene absorption in the visible range and the growth at *ca*. 340 nm of the naphthalenic component. (Bottom left) Extinction coefficients ε (M^{-1} cm^{-1}) of photodimers **D1** and **D3**, (bottom right) ε of photodimers **D2** and **D4** (MCH, RT)

rings. A less predictable observation is that the symmetric photodimers involving the positions 5,12 are not detected, whereas the other four combinations occur. This absence of photodimers **D5/D6** cannot be explained at this stage of our studies, and might tentatively be attributed to a lack of reactivity due to electronic effects or geometrical factors in the transition state (excimer-like species), or to a thermal instability of the photodimers **D5/D6** (as suggested by preliminary calculations[8]). By comparison, for the 5,12-DDOT, the cycloaddition involving the 5,12 positions did also not occur and only the photodimers involving the carbons 6,11 had been formed.[3a]

The quantum yields Φ_r reveal that the two *anti* photodimers are formed more efficiently than the two *syn* photodimers (ratio 60/40). This slightly higher reactivity is probably due to the propensity of the 2,3-DDOT to preorganize at low concentration due to a favorable head-to-tail dipole–dipole interaction.[3] In the gel phase, where the molecules are self-assembled into nanofibers,

Table 2. Photodimerization quantum yields (Φ_r, ±15%) of 2,3-DDOT (in fluid solution and in gel phase) and 5,12-DDOT at RT

	Solvent	Conc. (10^{-3} M) or rel. conc. (%)	Phase	Φ_r
5,12-DDOT	MCH	10	Sol.	6.5
2,3-DDOT	MCH	0.5	Sol.	5.9
2,3-DDOT-D1		(19 %)		1.1
2,3-DDOT-D2		(21%)		1.2
2,3-DDOT-D3		(29%)		1.7
2,3-DDOT-D4		(31%)[b]		1.8
2,3-DDOT	DMSO[a]	1.0	Gel	<0.2

For each photodimer obtained for 2,3-DDOT in MCH, Φ_r as well as relative concentration (in brackets) are reported.
[a] In fluid DMSO solution (0.1×10^{-3} M) the photoreactivity was found to be higher (*ca*. 0.02), but the photoproducts in DMSO have not been isolated and their respective distribution not established.
[b] Contains trace amounts of a fifth photoproduct.

DOI: 10.1002/poc

Φ_r is significantly reduced ($<2 \times 10^{-4}$, Table 2), involving a strong stabilization of the tetracene towards photoreactions. This is probably connected to the rigid and specific molecular packing within the fibers which impedes the photodimerization.[3b] In addition, rapid deactivation of the reactive excited states could be linked to efficient excitation energy transfer occurring within the fiber towards non-reactive energy traps.[9] As the sol–gel transition is thermo-reversible (sharp phase transition) and adjustable to room temperature, the system is of interest for combined photo- and thermochromic applications.

The strong photo-induced color change, from yellow-orange to non-colored, is a clear indication of the potential of these compounds as photochromic substances. In this, they result similar to the well-exploited anthracene derivatives, presenting the large advantage of an absorption in the visible wavelength range. This family of photochromic acenes can furthermore be extended to soluble di-substituted pentacenes, which display higher absorption wavelengths.[10]

EXPERIMENTAL SECTION

Irradiation and chromatography

The quantum yield of the 2,3-DDOT photodimerization was measured relatively to the photochemical reduction of $K_3Fe(C_2O_4)_3 \cdot 3H_2O$ (Parker actinometer).[11] Two samples of 2,3-DDOT were prepared in 1 mm optical cells, degassed by freeze-thaw cycles and then irradiated with a 2 kW xenon-lamp at 470 nm. The photosynthesis was performed in cyclohexane saturated with Ar and irradiated for 24 h with a 1000 W halogen lamp in Teflon capped glass reactor equipped with a magnetic stirrer (Duran glass: transmittance 5% at 285 nm, 10% at 290 nm). The volumes of the solution were determined by calibration of the height of solution in the cell and are calculated after the freeze-thaw procedure. The initial concentration is determined using the optical density of the solutions. The decrease in OD of the cells due to the photodimerization is taken into consideration. After the reaction, the solvent is evaporated under vacuum and the resulting mixture is separated, using column chromatography ('Kieselgel 60' (70–230 mesh), Merck KgaA (Darmstadt) under N2 pressure).

2,3-DDOT (600 mg, 1.11 mmol), cyclohexane (22 mL), solvent for chromatographic separation: DCM/ pentane (1:3) to pure DCM, further separation of the photodimers by several runs of column chromatography, solvent: 15% DCM/pentane to 25% DCM/ pentane. Besides 123 mg (21%) of 2,3-DDOT, the following photodimers were obtained as waxy, nearly colorless solids: D1: 61 mg (10%); D2: 67 mg (11%); D3: 85 mg (15%); D4 + fifth photoproduct (trace amounts): 94 mg (16%).

NMR and optical spectroscopy

IR spectroscopy. It was performed on KBr pellets on a Nicolet 320 FT-IR-spectrometer or on a diamond ATR spectrometer Bruker Tensor 27. The intensity of the bands is abbreviated with w (weak, up to 33% of the most intense band), m (medium, 34–67% of the most intense band), and s (strong, more than 68% of the most intense band).

UV/Vis absorption spectroscopy. In Braunschweig, Beckman UV 5230 spectrometer was used. As solvent, DCM of spectroscopic pure quality was used, unless otherwise stated. In Bordeaux, a Hitachi U-3300 spectrometer was used.

NMR spectroscopy. ^{1}H and ^{13}C NMR spectra were measured in deuterated chloroform using tetramethylsilane (TMS) as internal standard. The multiplicities are abbreviated as follows: s = singlet, d = doublet, t = triplet, q = quartet, m = multiplet, mc = multiplet center (used for higher order spin systems).

The coupling constants for the AA'XX'-spin system of some compounds were analyzed by iterative calculation, using the WinDAISY 4.1 software (Bruker Rheinstetten). R-factors are generally better than 0.85%. In the cases where the spin system was not calculated, the distance between the outer signals is given in Hz (*N*-values). The following spectrometers were used: Bruker AC 200: ^{1}H NMR (200.2 MHz), ^{13}C (50.3 MHz); Bruker DRX 400: ^{1}H NMR (400.1 MHz), ^{13}C (100.6 MHz).

D1: IR (ATR): $\nu = 2922\ cm^{-1}$ (s), 2853 (s), 1613 (w), 1505 (m), 1488 (w), 1462 (s), 1414 (w), 1386 (w), 1259 (s), 1195 (w), 1161 (s). **UV** (DCM): λ_{max} (lg ε) = 236 nm (5.03), 245 (5.02, sh), 305 (3.68), 321 (3.93), 336 (4.01).

^{1}H NMR (400 MHz, $CDCl_3$): $\delta = 7.20$ (s, 4 H, 12/5/12′5′-H), 6.94 (mc, $N = 8.6$ Hz, 4 H, 10/7/10′/7′-H), 6.81 (mc, $N = 8.7$ Hz, 4 H, 9/8/9′/8′-H), 6.80 (s, 4 H, 4/1/4′/1′-H), 4.74 (s, 4 H, 11/6/11′/6′-H), 3.94–3.91 (m, 8 H, 23/13/23′/13′-H), 1.80–1.77 (m, 8 H, chain), 1.44–1.42 (m, 8 H, chain), 1.31–1.26 (m, 32 H, chain), 0.89–0.86 (m, 12 H, 22/32/22′/32′-H). **^{13}C NMR** (100 MHz, $CDCl_3$): $\delta = 148.8$ (s, C-3/2/3′/2′), 143.6 (s, C-10a/6a/10a′/6a′), 139.2 (s, C-11a/5a/11a′/5a′), 127.5 (s, C-12a/4a/12a′/4a′), 127.0 (d, C-10/7/10′/7′), 125.6 (d, C-9/8/9′/8′), 124.0 (d, C-12/5/12′/5′), 107.9 (d, C-4/1/4′/1′), 68.7 (t, C-23/13/23′/13′), 53.9 (d, C-11/6/11′/6′), 31.9, 29.63, 29.58, 29.45, 29.35, 29.2, 26.1, 22.7 (t, chain), 14.1 (q, C-32/22/32′/22′).

D2: IR (ATR): $\nu = 2921\ cm^{-1}$ (s), 2852 (s), 1611 (w); 1502 (m), 1462 (m), 1415 (w), 1382 (w), 1307 (m), 1256 (s), 1187 (w), 1162 (m). **UV** (DCM): λ_{max} (lg ε) = 234 nm (4.38), 248 (4.32, sh), 274 (3.87, sh), 320 (3.19), 335 (3.29).

^{1}H NMR (400 MHz, $CDCl_3$): $\delta = 7.57$ (mc, $N = 9.4$ Hz, 2 H, 10/7-H), 7.35 (s, 2 H, 11/6-H), 7.27 (mc, $N = 9.4$ Hz, 2 H, 9/8-H), 7.20 (s, 2 H, 12′/5′-H),

DOI: 10.1002/poc

6.89–6.87 (m, 4 H, 4′/1′-H and 10′/7′-H), 6.62 (mc, $N = 8.6$ Hz, 2 H, 9′/8′-H), 6.51 (s, 2 H, 4/1-H), 4.69 (s, 2 H, 11′/6′-H), 4.68 (s, 2 H, 12/5-H), 4.03–3.99 (m, 4 H, 23′/13′-H), 3.72–3.68 (m, 4 H, 23/13-H), 1.91–1.82 (m, 4 H, chain), 1.59–1.44 (m, 8 H, chain), 1.37–1.25 (m, 52 H, chain), 0.90–0.86 (m, 12 H, 32/32′/22/22′-H). **^{13}C NMR** (100 MHz, CDCl3): 149.0 (s, C-3′/2′), 146.9 (s, C-3/2), 143.2 (s, C-10a′/6a′), 141.7 (s, C-11a/5a), 139.2 (s, C-11a′/5a′), 136.1 (s, C-12a/4a), 132.0 (s, C-10a/6a), 127.7 (s, C- 12a′/4a′), 127.10 (d, C-10/7), 127.05 (d, C-10′/7′), 125.6 (d, C-9′/8′), 124.93 (d, C-9/8), 124.88 (d, C-11/6), 123.9 (d, C-12′/5′), 115.1 (d, C-4/1), 108.0 (d, C-4′/1′), 69.9 (t, C-23/13), 68.9 (t, C-23′/13′), 53.9 (d, C-11′/6′), 53.5 (d, C-12/5), 31.9, 29.68, 29.65, 29.61, 29.5, 29.4, 29.38, 29.2, 29.16, 26.13, 29.09, 26.0, 22.7 (t, chain), 14.1 (q, C-32/32′/22/22′).

D3: IR (ATR): $\nu = 2956\ cm^{-1}$ (m), 2920 (s), 2852 (s), 1613 (w), 1501 (m), 1464 (m), 1406 (w), 1390 (w), 1251 (s), 1199 (m), 1158 (m), 1110 (m), 1014 (w). **UV** (DCM): λ_{max} (lg ε) = 255 nm (5.06), 320 (3.98), 336 (4.21).

^{1}H NMR (400 MHz, $CDCl_3$): $\delta = 7.12$ (s, 4 H, 12,5,12′,5′-H), 6.83 (mc, $N = 8.7$ Hz, 4 H, 10,7,10′,7′-H), 6.81 (s, 4 H, 4,1,4′,1′-H), 6.59 (mc, $N = 8.7$ Hz, 4 H, 9,8,9′,8′-H), 4.66 (s, 4 H, 11,6,11′,6′-H), 3.98–3.89 (m, 8 H, 23,13,23′,13′-H), 1.79–1.73 (m, 8 H, chain), 1.44–1.35 (m, 8 H, chain), 1.30–1.20 (m, 56 H, chain), 0.83–0.80 (m, 12 H, 32,22,32′,22′-H). **^{13}C NMR** (100 MHz, $CDCl_3$): $\delta = 148.8$ (s, C-3,2,3′,2′), 143.2 (s, C-10a,6a, 10a′,6a′), 139.4 (s, C-11a,5a,11a′,5a′), 127.5 (s, C-12a, 4a,12a′,4a′), 127.0 (d, C-10,7,10′,7′), 125.5 (d, C-9,8,9′,8′), 123.8 (d, C-12,5,12′,5′), 107.8 (d, C-4,1,4′,1′), 68.7 (t, C-23,13,23′,13′), 53.8 (d, C-11,6,11′,6′), 31.9, 29.6, 29.59, 29.5, 29.4, 29.2, 26.1, 22.7 (t, chain), 14.1 (q, C-32,22,32′,22′).

D4: IR (ATR): $\nu = 2922\ cm^{-1}$ (s), 2853 (s), 1612 (w); 1501 (s), 1462 (m), 1415 (w), 1382 (w), 1304 (m), 1257 (s), 1229 (s), 1161 (m), 1110 (w), 1080 (w). **UV** (DCM): λ_{max} (lg ε) = 232 nm (5.05), 320 (3.79), 329 (3.71), 337 (3.82).

^{1}H NMR (400 MHz, $CDCl_3$): $\delta = 7.49$ (mc, $N = 9.4$ Hz, 2 H, 10/7-H), 7.34 (s, 2 H, 11/6-H), 7.18-7.16 (m, 4 H, 9/8-H, and 12′/5′-H), 6.93 (mc, $N = 8.7$ Hz, 2 H, 10′/7′-H), 6.80 (mc, $N = 8.6$ Hz, 2 H, 9′/8′-H), 6.77 (s, 2 H, 4′/1′-H), 6.53 (s, 2 H, 4/1-H), 4.70 (s, 2 H, 11′/6′-H), 4.69 (s, 2 H, 12/5-H), 3.92 (t, $3J = 6.7$ Hz, 4 H, 23′/13′-H), 3.84–3.78 (m, 4 H, 23/13-H), 1.79–1.75 (m, 4 H, chain), 1.69–1.65 (m, 4 H, chain), 1.42–1.25 (m, 56 H, chain), 0.90–0.86 (m, 12 H, 32/22/32′/22′-H). **^{13}C NMR** (100 MHz, $CDCl_3$): $\delta = 148.7$ (s, C-3′/2′), 146.9 (s, C-3/2), 143.3 (s, C-10a′/6a′), 141.5 (s, C-11a/5a), 139.2 (s, C-11a′/5a′), 136.2 (s, C-12a/4a), 131.9 (s, C-10a/6a), 127.5 (s, C-12a′/4a′), 127.1 (d, C-10/7), 126.9 (d, C-10′/7′), 125.7 (d, C-9′/8′), 125.0 (d, C-11/6), 124.9 (d, C-9/8), 124.0 (d, C-12′/5′), 114.9 (d, C-4/1), 107.8 (d, C-4′/1′), 69.9 (t, C-23/13), 68.7 (t, C-23′/13′), 53.9 (d, C-11′/6′), 53.5 (d, C-12/5), 31.9, 29.65, 29.61, 29.56, 29.43, 29.41, 29.36, 29.34, 29.26, 29.1, 26.04, 25.96, 25.87, 22.7 (t, chain), 14.1 (q, C-32/22/32′/22′).

Acknowledgements

We wish to thank Pr. Henri Bouas-Laurent for his input in this project and acknowledge his outstanding contribution to research on photochromism. This research was financially supported by the 'Ministère de la Recherche', the CNRS, the Région Aquitaine, and the Fonds der Chemischen Industrie for financial assistance.

REFERENCES

1. (a) Bouas-Laurent H, Desvergne JP. In *Photochromism, Molecules and Systems* (revised edn), Dürr H, Bouas-Laurent H (eds). Elsevier: Amsterdam, The Netherlands, 2003; (b) Bouas-Laurent H Castellan A Desvergne JP Lapouyade R *Chem. Soc. Rev.* 2000; **29**: 43–55; (c) Bouas-Laurent H, Castellan A, Desvergne JP, Lapouyade R. *Chem. Soc. Rev.* 2001; **30**: 248–263; (d) Fudickar W, Linker T. *Chem. Eur. J.* 2006; **12**: 9276–9283.
2. Bouas-Laurent H, Dürr H. *Pure Appl. Chem.* 2001; **73**: 639–665.
3. (a) Reichwagen J, Hopf H, Del Guerzo A, Desvergne JP, Bouas-Laurent H. *Org. Lett.* 2004; **6**(12): 1899–1902; (b) Reichwagen J, Hopf H, Del Guerzo A, Belin C, Desvergne JP, Bouas-Laurent H. *Org. Lett.* 2005; **7**(6): 971–974; (c) Del Guerzo A, Desvergne JP, Bouas-Laurent H, Belin C, Reichwagen J, Hopf H. *Mol. Cryst. Liq. Cryst.* 2005; **431**: 155/455–159/459.
4. (a) Odon SA, Parkin SR, Anthony JE. *Org. Lett.* 2003; **5**: 4245–4248; (b) Anthony JE, Eaton DL, Parkin SR. *Org. Lett.* 2002; **4**: 15–18; (c) Brinkmann M, Graff S, Straupé C, Wittmann JC, Chaumont C, Nuesch F, Aziz A, Schaer M, Zuppiroli L. *J. Phys. Chem B* 2003; **107**: 10531–10539; (d) Nichols JA, Gundlach DJ, Jackson TN. *Appl. Phys. Lett.* 2003; **83**: 2366–2368; (e) Kitamura M, Imada T, Arakawa Y. *Appl. Phys. Lett.* 2003; **83**: 3410–3412.
5. Photodimers tend to decompose into monomers under the experimental conditions of the analyses.
6. Birks JB. *Photophysics of Aromatic Compounds*. Wiley Interscience: New York, 1970.
7. Fages F, Desvergne JP, Frisch I, Bouas-Laurent H. *J. C. S. Chem. Commun.* 1988; 1413–1415.
8. Preliminary studies performed by semi-empirical PM3 calculations of heat of formations of the *anti* photodimers of 2,3-dimethoxytetracene in vacuum (using CACHE—MOPAC software) indicate that the structure equivalent to **D6** is 2.5 kcal/mol less stable than **D3** and 1.5 kcal/mol less stable than **D4**. This suggests that **D6** would more likely thermally reverse to the monomer during the irradiation.
9. Del Guerzo A, Olive AGL, Reichwagen J, Hopf H, Desvergne JP. *J. Am. Chem. Soc.* 2005; **127**: 17984–17985.
10. (a) Reichwagen J, Hopf H, Desvergne JP, Del Guerzo A, Bouas-Laurent H. *Synthesis* 2005; **20**: 3505–3507; (b) Desvergne JP, Del Guerzo A, Bouas-Laurent H, Belin C, Reichwagen J, Hopf H. *Pure Appl. Chem.* 2006; **78**(4): 707–720.
11. Hatchard CG, Parker CA. *Proc. R. Soc. Lond. A* 1956; **235**: 518–535.

DOI: 10.1002/poc